

## Role of Phenyl Radicals in the Growth of Polycyclic Aromatic Hydrocarbons

Bikau Shukla, Akio Susa, Akira Miyoshi, and Mitsuo Koshi\*

Department of Chemical System Engineering, The University of Tokyo, 7-3-1, Bunkyo-ku, Hongo, Tokyo, 113-8656, JAPAN

Received: October 9, 2007; In Final Form: December 11, 2007

To investigate the role of phenyl radical in the growth of PAHs (polycyclic aromatic hydrocarbons), pyrolysis of toluene with and without benzene has been studied by using a heatable tubular reactor couple with an in-situ sampling vacuum ultraviolet (VUV) single photon ionization (SPI) time-of-flight mass spectrometer (TOFMS) at temperatures 1155–1467 K and a pressure of 10.02 Torr with 0.56 s residence time. When benzene was added, a significant increase of phenyl addition products (biphenyl, terphenyl, and triphenylene) was observed and the mass spectra showed a clear regular sequence with an interval of  $\sim 74$  mass number, corresponding to the phenyl addition ( $+C_6H_5$ ) followed by H-elimination ( $-H$ ) and cyclization ( $-H_2$ ). The analysis showed that the PAC (phenyl addition/cyclization) mechanism is efficient for the growth of PAHs without a triple fusing site, for which the HACA (hydrogen abstraction/ $C_2H_2$  addition) step is inefficient, and produces PAHs with five-membered rings. The PAC process was also suggested to be efficient in the subsequent growth of PAHs with five-membered rings. The role of the PAC mechanism in combustion conditions is discussed in relation to the importance of disordered five-membered ring structure in fullerene or soot core.

### Introduction

Although it has been widely accepted that gaseous PAHs (polycyclic aromatic hydrocarbons) are precursors of soot particles formed in combustion,<sup>1</sup> until now, no attempt has been successful to clarify the size of PAHs at which their rate of coalescence exceeds the rate of growth. The mechanism of first aromatic ring formation is fairly well-known<sup>2,3</sup> whereas the mechanisms of large PAHs formation are unclear.<sup>4</sup> Bockhorn et al.<sup>5</sup> proposed the HACA (hydrogen abstraction and acetylene addition) mechanism for the formation and growth of PAHs that was further modified by Frenklach et al.<sup>6</sup> However, later, Bohm et al.<sup>7</sup> and McKinnon et al.<sup>8</sup> indicated that the HACA mechanism is too slow to explain the fast experimental PAHs and soot formations, as it increases the mass of species by only 24 u in each step. Though assumed in many models, it is still unclear whether coronene or pyrene is sufficient for coagulation precursor into the fine soot particle ( $\sim 2000$  u) or not. Some recent studies<sup>9</sup> detected PAHs greater than coronene.

As an alternative fast process, Bohm et al.<sup>7</sup> proposed aromatic ring–ring condensation and acetylene addition mechanism. The aryl–aryl combination followed by  $H_2$ -elimination and ring cyclization have been also suggested in many studies.<sup>10</sup> Condensation of aromatic radical with neutral species has been also proposed by Unterreiner et al.<sup>11</sup> The DFT calculations showed that the energy barrier was below  $100 \text{ kJ mol}^{-1}$  and decreased with increasing size of the radicals. Benzene or phenyl has been reported to produce non-benzenoid PAHs such as fluoranthene, benzo[*b*]fluoranthene and indeno[1,2,3-*cd*]pyrene through one step reactions with naphthalene, phenanthrene, and pyrene.<sup>12</sup>

In the previous study,<sup>13</sup> it was found that addition of acetylene rather diminishes the growth of PAHs in the pyrolysis of toluene,

and the important roles of addition reactions of phenyl radical to PAHs in their growth was suggested. In the present study, to investigate the suggested roles of phenyl radicals in detail, gas-phase products observed in the pyrolysis of toluene + benzene mixtures were compared to those observed in the pyrolysis of toluene only.

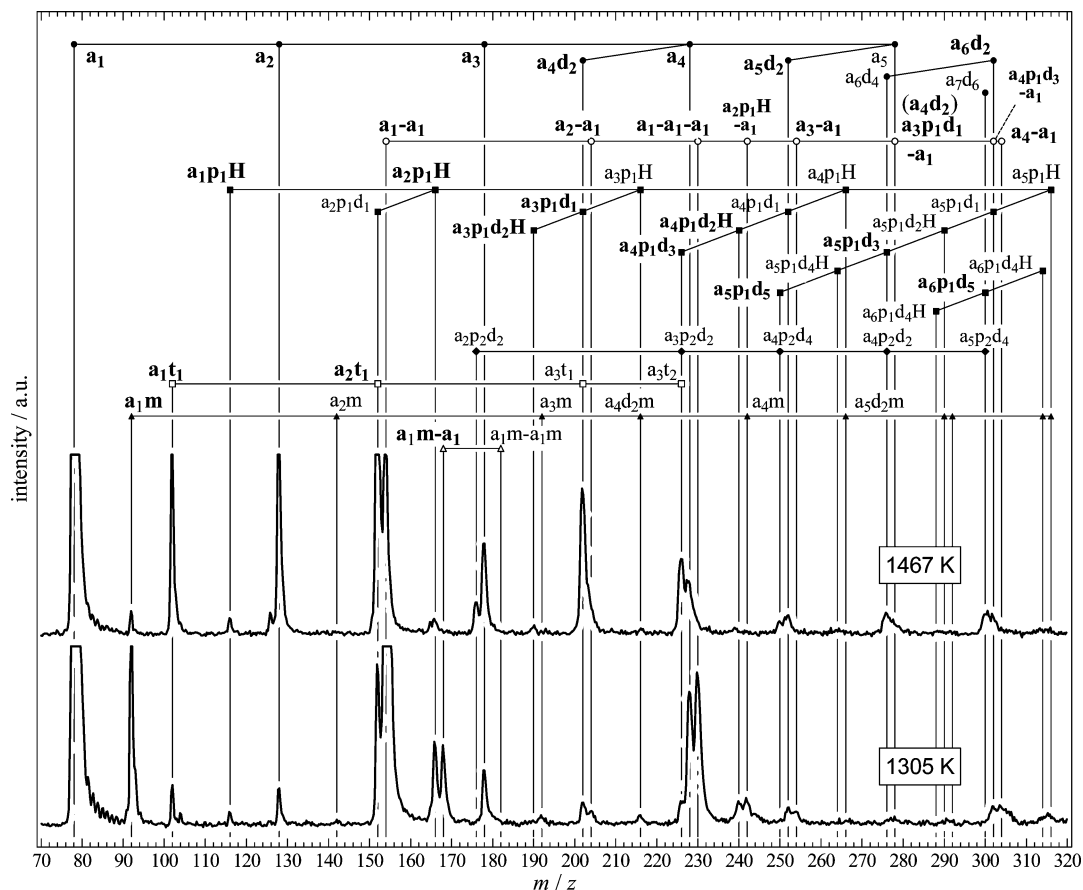
### Experimental Section

Details of the experimental setup have been described elsewhere.<sup>13</sup> Briefly, the apparatus consists of a quartz reaction tube wrapped with a tungsten heater placed into a source chamber aligned with the linear TOFMS. A UV laser pulse (355 nm) was loosely focused into the frequency tripling cell filled with xenon (pressure = 7.41 Torr) to generate VUV photons at 118 nm (10.5 eV). The UV beam was separated and removed by a LiF crystal prism to avoid the  $(1 + 1)$  ionization by 355 and 118 nm photons.

A premixture of 40% toluene in He or 20% toluene and 20% benzene in He was supplied through a mass flow controller into the quartz reaction tube. The gaseous product molecules were continuously sampled through a pinhole and were collimated by a 1.0 mm orifice skimmer mounted at 3.0 mm from the pinhole. The molecular beam was introduced into the ionization region of the TOFMS and the molecular species were ionized by the 118 nm photons. The ionized species were accelerated by the electrodes, electronic lenses and deflectors through the [field-free] drift tube to the MCP (multichannel plate). Mass spectra were recorded at different temperatures (1155–1467 K) at constant pressure (10.02 Torr) and constant residence time (0.56 s).

The electron impact ionization by photoelectrons produced by stray light or the multiphoton ionization that may cause fragmentation was ruled out by the absence of signal from the species with IP's greater than 10.5 eV and absence of fragment

\* Corresponding author. Phone: +81-3-5841-7295, Fax: +81-3-5841-7488. E-mail: koshi@chemsys.t.u-tokyo.ac.jp.



**Figure 1.** PAHs assignment of mass spectra for toluene + benzene mixture pyrolysis products at 1305 and 1467 K. The symbol  $a_n p_l t_k d_m$  denotes fused PAHs consisting of  $n$  hexagonal,  $l$  pentagonal, and  $k$  tetragonal rings with  $m$  internal carbon (see text for details).

ions. The reaction tube was cleaned every time before the experiment to avoid the contamination from the condensate substances, although tarry condensate was observed only outside the heating zone in the downstream direction. Laser power dependence was checked before the experiments to avoid fragmentation due to multiphoton ionization.

## Results

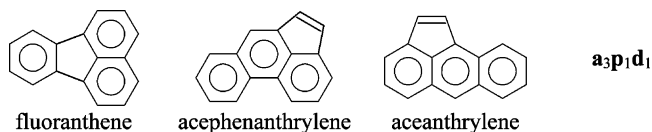
The previous notations<sup>13</sup> of regular sequence of PAHs in the mass spectra have been extended in the present study for the generalized representation of PAHs with five or four-membered rings. Fused PAHs with 6-, 5-, and 4-membered rings are designated as

$$a_n p_l t_k d_m [H] \quad (1)$$

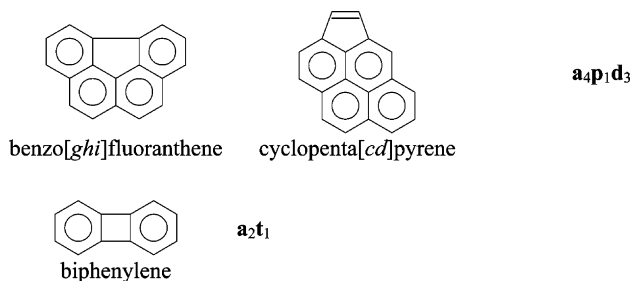
where  $n$ ,  $l$ , and  $k$  are the numbers of hexagonal (**a**), pentagonal (**p**), and tetragonal (**t**) rings and  $m$  is the number of internal carbon atoms. Their chemical formulas are

$$C_2H_4 + n(C_4H_2) + l(C_3H_1) + k(C_2) - m(C_1H_1) + [H] \quad (2)$$

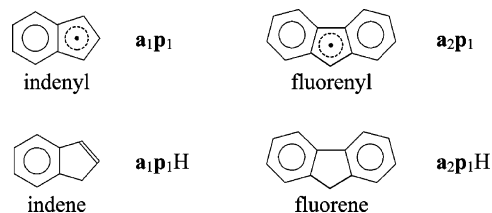
For example,  $a_3 p_1 d_1$  ( $C_{16}H_{10}$ ) represents fluoranthene, acephenanthrylene, aceanthrylene, etc.



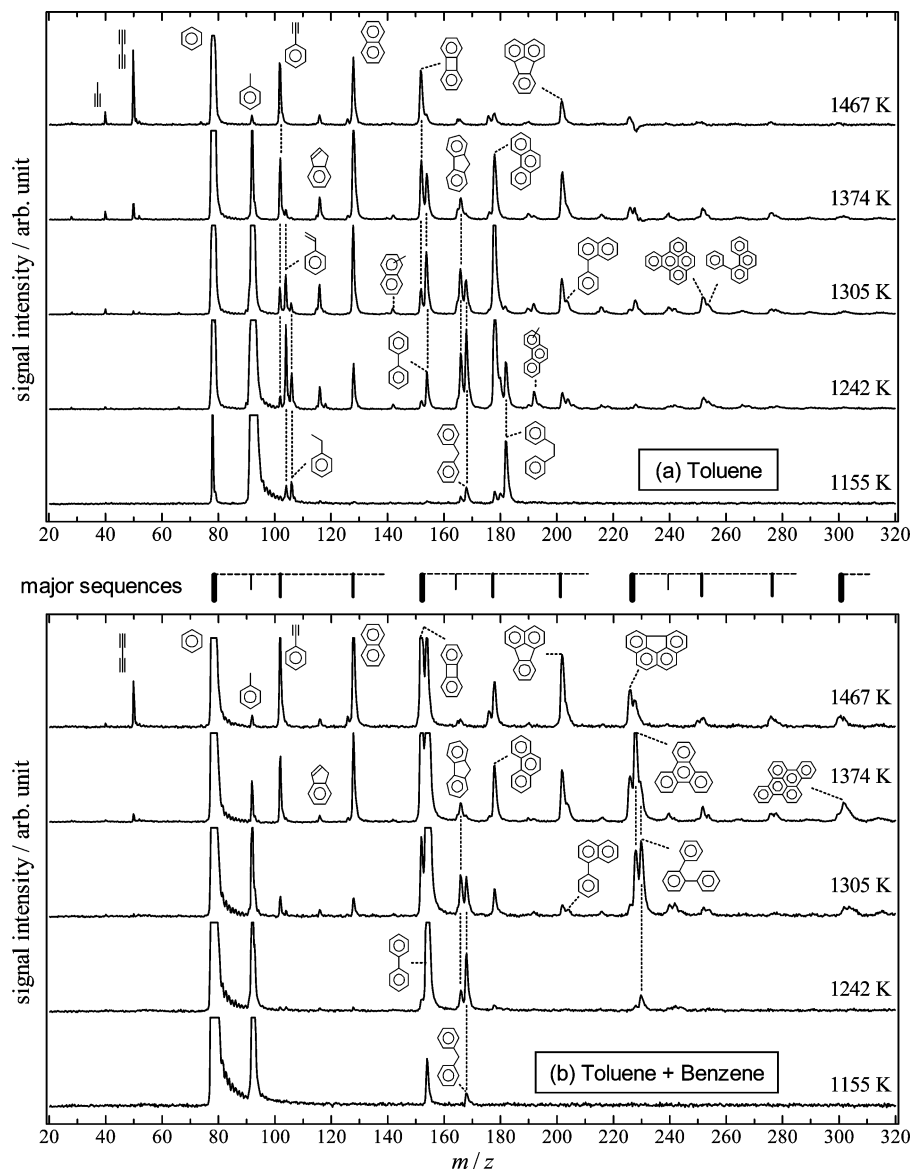
The latter two have been denoted as  $a_3 c_1$  in the previous report.<sup>13</sup> Similarly,  $a_4 p_1 d_3$  ( $C_{18}H_{10}$ ) denotes benzo[ghi]fluoranthene, cyclopenta[cd]pyrene, etc., and  $a_2 t_1$  ( $C_{12}H_8$ ) denotes biphenylene.



It should be noted that, when  $l + m$  is odd, the number of hydrogen atoms is odd and the notation represents delocalized radicals such as indenyl ( $a_1 p_1$ ) or fluorenyl ( $a_2 p_1$ ), and corresponding compounds with one more hydrogen such as indene ( $a_1 p_1 H$ ) or fluorene ( $a_2 p_1 H$ ).



Nonfused compounds are denoted as  $a_1 - a_3$  or  $a_2 m$ , etc. similarly to the previous report.<sup>13</sup>



**Figure 2.** Product mass spectra of (a) toluene pyrolysis and (b) toluene + benzene pyrolysis at five different temperatures and at a pressure of 10.02 Torr. Observed regular sequences with  $\sim 74$  mass number interval are shown on top of frame (b).

**Mass Peak Assignment.** The notations described above were used to list the possible compounds corresponding to the mass numbers exhaustively. Figure 1 shows product mass spectra of toluene + benzene pyrolysis with all the mass positions of fused PAHs of hexagonal rings only ( $\mathbf{a}_n\mathbf{d}_m$ ) and those of one pentagonal ring ( $\mathbf{a}_n\mathbf{p}_1\mathbf{d}_m[\text{H}]$ ). Selected relevant mass positions of phenyl substituted ( $\mathbf{a}_n\mathbf{p}_1\mathbf{d}_m[\text{H}]-\mathbf{a}_1$ ) and methyl substituted ( $\mathbf{a}_n\mathbf{d}_m\mathbf{m}$  and  $\mathbf{a}_1\mathbf{m}-\mathbf{a}_1[\mathbf{m}]$ ) PAHs, PAHs with tetragonal rings ( $\mathbf{a}_n\mathbf{t}_k$ ), and PAHs with two pentagonal rings ( $\mathbf{a}_n\mathbf{p}_2\mathbf{d}_2$ ) are also shown. Most of the mass peaks of phenyl substituted PAHs ( $\mathbf{a}_n\mathbf{p}_1\mathbf{d}_m[\text{H}]-\mathbf{a}_1$ ) are found at the highest end of the same-carbon-number block of peaks without overlapping, and they were found to increase significantly by the addition of benzene. Also, compounds with small molecular weights such as  $\mathbf{a}_1\mathbf{p}_1\mathbf{H}$ ,  $\mathbf{a}_2$ ,  $\mathbf{a}_2\mathbf{p}_1\mathbf{H}$ , and  $\mathbf{a}_3$  could be identified uniquely. For larger molecules, there are increasing numbers of candidates for a mass peak and the identification was made with the help of the suggested chemical kinetics, which will be discussed in detail in the Discussion.

**Changes in Mass Spectra by Benzene Addition.** The mass spectra observed in toluene + benzene pyrolysis (b) are

compared with those for toluene only (a) in Figure 2 and the assignment of mass peaks is shown in Table 1. The addition of benzene significantly increases the intensities of biphenyl ( $\mathbf{a}_1-\mathbf{a}_1$ ,  $m/z = 154$ ) and terphenyl ( $\mathbf{a}_1-\mathbf{a}_1-\mathbf{a}_1$ ,  $m/z = 230$ ) whereas the low-temperature products that were suggested to be formed from benzyl radical in the previous study<sup>13</sup> (104:styrene, 106: ethylbenzene, 116:indene, 182:biphenyl) were found to be significantly depleted. These results suggest that the chain carriers X (=H, CH<sub>3</sub>, etc.), which produce benzyl by (R1) in toluene pyrolysis, react with benzene and form phenyl radicals (R2) in the toluene/benzene mixture. As shown at the top of

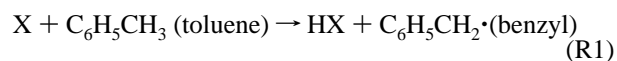
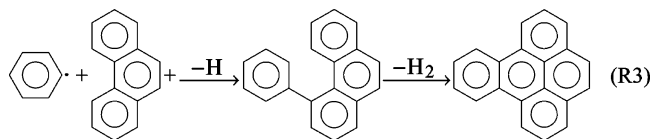
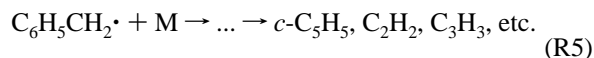
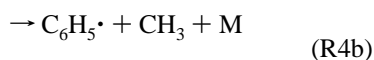


Figure 2b, the mass spectra of benzene + toluene pyrolysis shows regular repetition of sequences with an interval of  $\sim 74$  mass numbers, which corresponds to the addition of phenyl radical ( $\Delta m = +77$ ) followed by H-atom elimination ( $-1$ ) and cyclization ( $-2$ ), for example,



This suggests the importance of phenyl addition/cyclization (hereinafter abbreviated as PAC) processes in the growth of PAHs.

**Temperature Dependence of Mass Spectra.** Similarly to our previous report,<sup>13</sup> the greatest production of large PAHs was observed at temperature around 1374 K and it was diminished as the temperature either increased or decreased. Figure 3 shows the temperature variations of the intensities of strong peaks, which are out of scale in Figure 2. At around 1374 K, where growth of PAHs is efficient, most of the toluene reagent was found to be consumed and is suggested to be acting as the major source of active species (benzyl, phenyl, H, CH<sub>3</sub>, C<sub>2</sub>H<sub>2</sub>, C<sub>3</sub>H<sub>3</sub>, *c*-C<sub>5</sub>H<sub>5</sub> etc.) via the decomposition reactions,

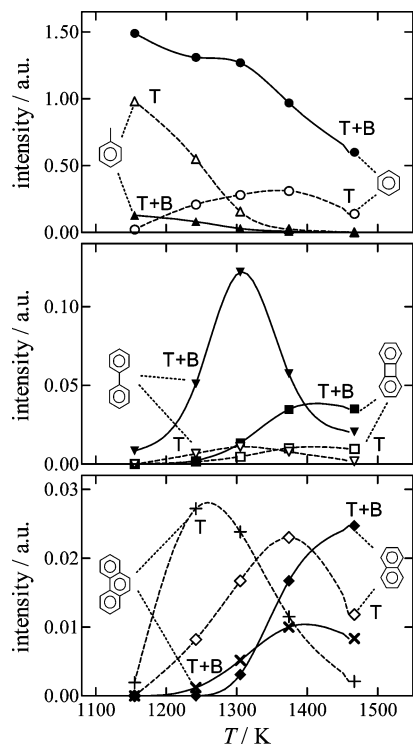


In contrast, significant amount of benzene in the mixture remains unreacted even at the highest temperature (1467 K) reflecting the smaller rate constant for thermal self-decomposition. The peak temperatures for the production of naphthalene and phenanthrene, as shown in the bottom frame of Figure 3, were found to shift higher by the addition of benzene, since these compounds are formed dominantly via benzyl radicals in pyrolysis of toluene, but via phenyl radicals when benzene was added. Even with the benzene, inhibition of PAHs formation was observed at the highest temperature (1467 K), which can be partly ascribed to the decrease of benzene, and also to the decrease of important intermediate, biphenyl, at high temperatures due to its conversion to less reactive biphenylene, as shown in the middle frame of Figure 3.

## Discussion

In this section, the expected reaction kinetics as well as the discussions on the assignment of mass peaks will be described from low temperature to high temperature, and at the last, the suggested roles of phenyl radicals in the PAHs formation in combustion will be discussed.

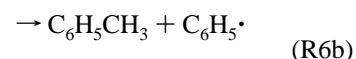
**Reaction Kinetics at Low Temperatures.** At lower temperatures, 1155 and 1242 K, in the pyrolysis of toluene, most of the observed products can be assigned to the recombination products of intermediates originating from toluene as described in the previous report.<sup>13</sup> Briefly, the mass peak at  $m/z = 106$  (C<sub>8</sub>H<sub>10</sub>) is assigned to ethylbenzene formed via the recombination of benzyl radical with CH<sub>3</sub>, and the neighboring peaks at  $m/z = 104$  and 102 can be estimated to be the successive H<sub>2</sub>-elimination products, styrene and phenylacetylene. Similarly, indene ( $m/z = 116$ ) is formed from benzyl + C<sub>2</sub>H<sub>2</sub>, naphthalene ( $m/z = 128$ ) from benzyl + C<sub>3</sub>H<sub>3</sub> and *c*-C<sub>5</sub>H<sub>5</sub> + *c*-C<sub>5</sub>H<sub>5</sub>, diphenylmethane ( $m/z = 168$ ) from benzyl + benzene/phenyl, bibenzyl ( $m/z = 182$ ) from benzyl + benzyl, and fluorene ( $m/z = 166$ ) and phenanthrene ( $m/z = 178$ ) from successive hydrogen atom elimination from diphenylmethane and bibenzyl. Also



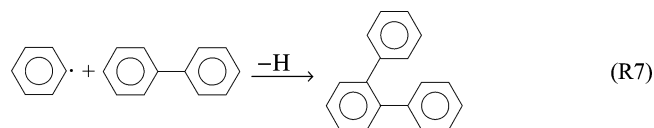
**Figure 3.** Temperature variation of the intensities of large mass peaks observed in the pyrolysis of toluene (T) and toluene/benzene mixture (T+B). Top frame: (○, ●) benzene, (△, ▲) toluene. Middle frame: (□, ■) biphenylene, (▽, ▼) biphenyl. Bottom frame: (◇, ◆) naphthalene, (+, ×) phenanthrene.

weak peaks of methyl substituted PAHs, methylnaphthalene ( $m/z = 142$ ) and methylphenanthrene ( $m/z = 192$ ) were observed.

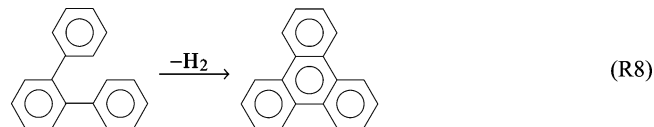
Almost all of these compounds disappeared by the addition of benzene except for biphenyl and diphenylmethane. As described in the previous section, the main reason for this seems to be the depletion of benzyl radicals due to reaction of atoms or radicals with benzene (R2). This is also consistent with the enhanced production of biphenyl ( $m/z = 154$ ) and the start of the production of terphenyl ( $m/z = 230$ ) due to the increase in concentration of phenyl radicals. Though the production of benzyl radicals by abstraction reaction (R1) is diminished, exceptional formation of diphenylmethane from the reaction of benzyl radicals with benzene (R6a) was observed. This is probably due to the benzyl radicals formed from the decomposition of toluene (R4a) and because the conversion of benzyl to phenyl via (R6b) is slow at lower temperatures.



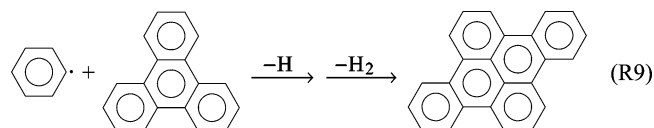
**Reaction Kinetics at High Temperatures.** At temperatures above ~1300 K, in the pyrolysis of toluene + benzene mixture, a large peak of biphenyl ( $m/z = 154$ , a<sub>1</sub>-a<sub>1</sub>) was observed together with the product at smaller mass number by 2 ( $m/z = 152$ ). Candidates at this mass number are acenaphthylene (a<sub>2</sub>p<sub>1</sub>d<sub>1</sub>) and biphenylene (a<sub>2</sub>t<sub>1</sub>). Considering the fact that, at 1305 K, this compound is formed more efficiently in the presence of benzene and the peak of naphthalene is much smaller than the case without benzene, this was ascribed to be biphenylene produced by the dehydrogenation of biphenyl. At this temperature range, significant formation of terphenyl ( $m/z = 230$ , a<sub>1</sub>-a<sub>1</sub>-a<sub>1</sub>), product of the phenyl addition to biphenyl, (R7)



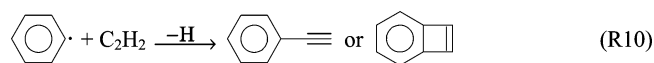
was also observed with dehydrogenated, 2-mass smaller, product. Though no significant site preference can be expected in the initial phenyl addition leading to three isomers (*o*-, *m*-, and *p*-terphenyl, as shown in Table 1), efficient dehydrogenation is expected only for the ortho isomer, which produces triphenylene ( $m/z = 228$ ) via (R8), and the reversible phenyl addition process will finally result in the dominant formation of *o*-terphenyl.



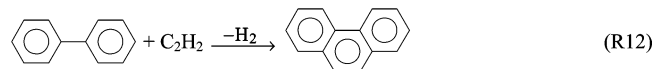
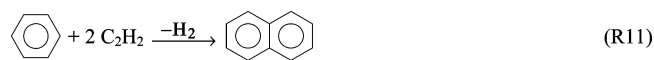
Compounds at  $m/z \sim 302$ , which are expected to be the products of further PAC (phenyl addition/cyclization) growth, were also found in the mass spectra, but their identification was not very certain.



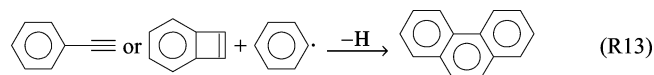
The mass peak at  $m/z = 102$  appeared only at high-temperature (1374 and 1467 K) when benzene was added, and it is assigned to phenylacetylene or bicyclo[4.2.0]octa-1,3,5,7-tetraene. In the case of toluene-only pyrolysis, it is formed from ethylbenzene; however, ethylbenzene was absent in the mixture pyrolysis,  $m/z = 102$  is formed by the reaction of phenyl radical with acetylene (R10).



For similar reasons, naphthalene and phenanthrene are expected to be formed via HACA processes from benzene (R11) and biphenyl (R12), respectively. The formation mechanisms of these compounds are apparently different from those formed in the pyrolysis of toluene-only at lower temperature.

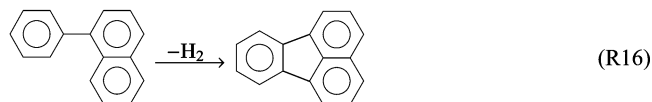
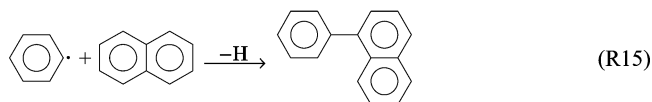
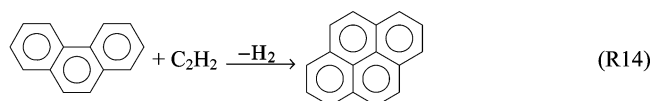


From the regular sequence of the mass spectra with mass  $\sim 74$  interval, formation of  $\mathbf{a}_3$  (phenanthrene) from  $\mathbf{a}_1\mathbf{t}_1$  is also suggested,<sup>2,14</sup> but no clear evidence for this reaction was found.



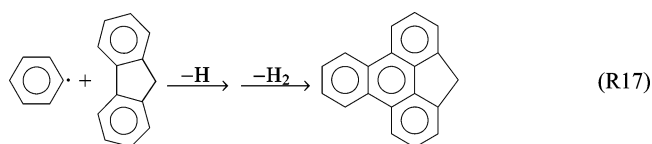
The mass peak at  $m/z = 202$  can be either pyrene ( $\mathbf{a}_4\mathbf{d}_2$ ) or fluoranthene ( $\mathbf{a}_3\mathbf{p}_1\mathbf{d}_1$ ) formed by the following reactions R14–R16.

From the mass  $\sim 74$  interval regular sequence and existence of  $m/z = 204$  peak, the latter is supported but the former is also

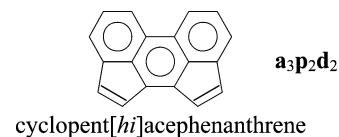


highly probable. As a general trend, mass peaks corresponding to phenyl substituted PAHs accompany  $-2$  mass number peaks that can be assigned to the cyclization products. These  $-2$  mass number peaks increase as temperature increases, indicating the stability of cyclization product compared to the phenyl substituted PAHs.

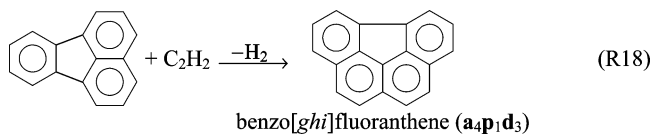
Though the intensity was smaller compared to those described above, the mass peak at  $m/z = 240$  can be ascribed to 4*H*-cyclopenta[*def*]triphenylene, that is, the PAC product from fluorene ( $m/z = 166$ ).



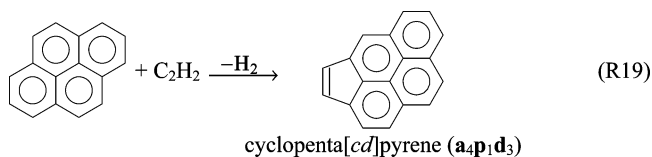
At temperatures 1374 and 1467 K, a mass peak corresponding to the dehydrogenation product ( $m/z = 226$ ) of triphenylene ( $m/z = 228$ ) was observed in benzene + toluene pyrolysis. It may be the dehydrogenated product ( $\mathbf{a}_3\mathbf{t}_2$ ) from *m*-terphenyl,  $\mathbf{a}_3\mathbf{p}_2\mathbf{d}_2$  (e.g., cyclopenta[*hi*]acephenanthrene), or  $\mathbf{a}_4\mathbf{p}_1\mathbf{d}_3$ .



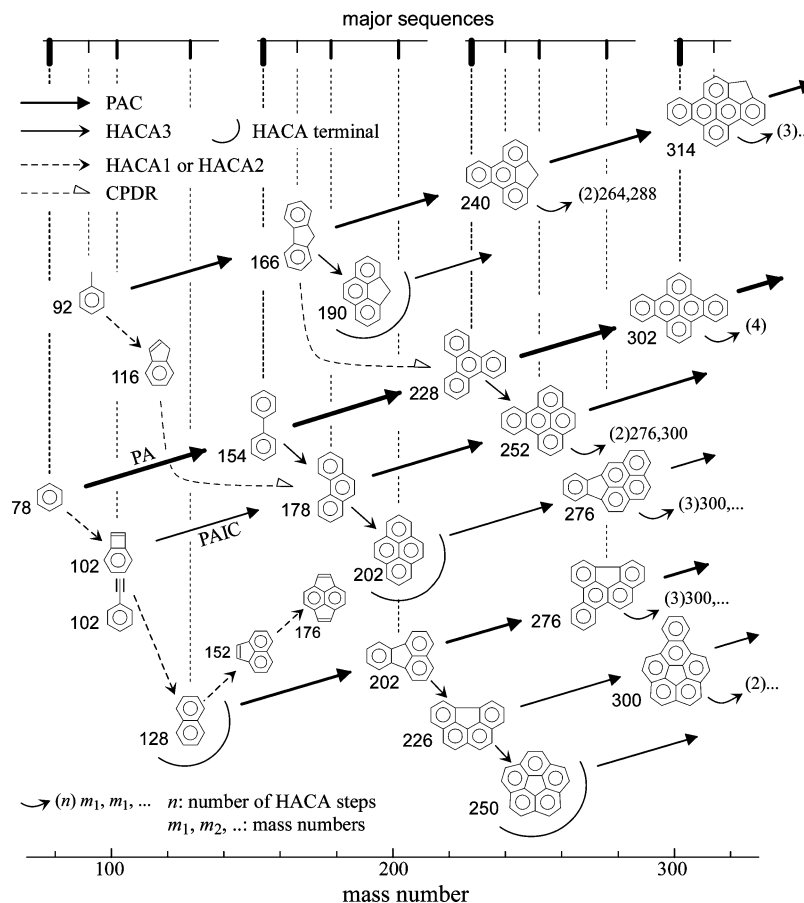
The most probable isomer of  $\mathbf{a}_4\mathbf{p}_1\mathbf{d}_3$  compound is benzo[*ghi*]fluoranthene produced by HACA from fluoranthene.



However, the contribution of the thermodynamically most stable isomer, cyclopenta[*cd*]pyrene, formed via HACA from pyrene may also be significant.



Also, at the highest temperature, a peak at mass number of 176 (phenanthrene  $- 2$ ) was observed and was attributed to pyracylene ( $\mathbf{a}_2\mathbf{p}_2\mathbf{d}_2$ ; see Table 1) on the basis of the analysis shown in Figure 1.



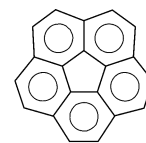
**Figure 4.** Suggested reaction mechanism of toluene + benzene pyrolysis. Bold-headed arrows denote PAC (phenyl addition/cyclization) processes, thin-headed arrows denote HACA processes at triple fusing sites (HACA3; with solid lines) or at single/double fusing sites (HACA1 and HACA2; with broken lines), and open-headed arrows denote CPDR (cyclopentadienyl radical recombination) processes. “PA” denotes phenyl addition only and “PAIC” denotes phenyl addition/isomerization/cyclization. The numbers at the bottom left of the structures are their mass numbers, and numbers with warped-up thin arrows in the form “(n)  $m_1, m_2, \dots$ ” are numbers of following HACA processes (n) and mass numbers of subsequent PAHs ( $m_1, m_2, \dots$ ). The regular sequences with an interval of  $\sim 74$  mass number are indicated at the top.

**Role of PAC (Phenyl Addition/Cyclization) Mechanism in Combustion.** Figure 4 outlines the major PAHs growth routes suggested for toluene + benzene pyrolysis investigated in this study. The PAC routes are indicated by thick-headed arrows in up-right direction and efficient HACA3 (HACA at triple fusing site) processes by thin-headed arrows in down-right direction. Several HACA1 and HACA2 (HACA at single and double fusing sites) suggested in the present study are also indicated by broken thin-headed arrows.

As can be seen from the figure, efficient HACA3 routes end at round shaped PAHs after several steps, and at the condition like in the pyrolysis of toluene + acetylene pyrolysis shown in the previous study,<sup>13</sup> after small number of HACA2, the growth stops at the structure like pyracylene. Though not efficient in toluene/benzene pyrolysis, CPDR (cyclopentadienyl radical recombination) growth may play some role for further growth. In the toluene + benzene system PAC routes for PAH growth appear in addition to the HACA and CPDR mechanisms. The signature of the PAC route is the regular sequence of mass spectra with  $\sim 74$  mass unit intervals. Because the structures of the PAC products usually have several triple-fusing sites, they allow further growth by HACA3. As a result, the most efficient growth of PAHs was observed at the condition ( $\sim 1374$  K) where both HACA and PAC mechanisms are active. Although the growth routes for small PAHs are rather specific to the starting compounds, the continuous sequence toward larger PAHs shown

here seems to be valuable for PAHs formation in various combustion or pyrolytic conditions.

Another interesting feature of PAC mechanism is that it produces PAHs with five-membered ring when the phenyl addition occurs at a double fusing site, and it is also efficient for the subsequent growth of PAHs with five-membered rings. Corannulene (mass number: 250) is a typical example of the PAHs with five-membered ring grown by PAC.



$a_5p_1d_5$

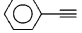

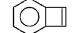
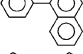
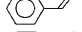

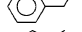
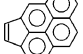
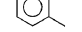
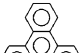
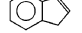
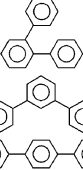
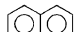

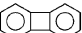
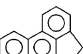

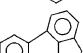
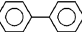
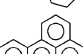
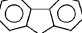
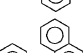
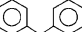
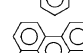
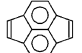
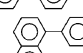
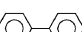


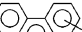
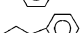
dibenzo[*ghi,mno*]fluoranthene or corannulene

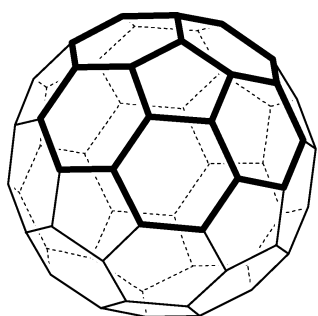
It is a part of  $C_{60}$  fullerene structure, as shown in Figure 5, and thus nonplanar. Also the five-membered ring is an essential component of the curved graphene layers observed in soot particles in the core region.<sup>15</sup> The role of PAC in the production of fullerenes as well as the soot will be an interesting subject for future studies.

## Conclusion

To investigate the phenyl addition/cyclization (PAC) growth mechanism suggested in our previous study,<sup>13</sup> products of toluene + benzene pyrolysis were detected by the VUV-SPI-

**TABLE 1: Assignment of Major Products and Suggested Precursors in the Pyrolysis of Toluene and Toluene + Benzene Mixture**

<i>m/z</i>	assigned compound	suggested precursor(s)	<i>m/z</i>	assigned compound	suggested precursor(s)
102	phenylacetylene	 $\text{C}_6\text{H}_5\text{C}\equiv\text{CH}$ / $\text{C}_6\text{H}_5\text{C}\equiv\text{C}\cdot$ + $\equiv$ (-H)		pyrene	 + $\equiv$ (-H <sub>2</sub> )
	bicyclo[4.2.0]octa-1,3,5,7-tetraene	 + $\equiv$ (-H)	204	phenylnaphthalene	 + $\text{C}_6\text{H}_5\cdot$ (-H)
104	styrene	 (-H <sub>2</sub> )	226	benzo[ghi]fluoranthene	 + $\equiv$ (-H <sub>2</sub> )
106	ethylbenzene	 + CH <sub>3</sub>		cyclopenta[cd]pyrene	 + $\equiv$ (-H <sub>2</sub> )
	xylene	 + CH <sub>3</sub> (-H)	228	triphenylene	 (-H <sub>2</sub> )
116	indene	 + $\equiv$ (-H)	230	<i>o</i> -terphenyl	 + $\text{C}_6\text{H}_5\cdot$ + $\text{C}_6\text{H}_4\cdot$ (-H)
128	naphthalene	 + $\cdot$ + $\equiv$ (-H <sub>2</sub> )		<i>m</i> -terphenyl	
142	methylnaphthalene	 + CH <sub>3</sub> (-H)		<i>p</i> -terphenyl	
152	biphenylene	 (-H <sub>2</sub> )	240	4H-cyclopenta[def]triphenylene	 (-H <sub>2</sub> )
	acenaphthylene	 + $\equiv$ (-H <sub>2</sub> )	242	phenylfluorene	 + $\text{C}_6\text{H}_5\cdot$ + $\text{C}_6\text{H}_4\cdot$ (-H)
154	biphenyl	 + $\text{C}_6\text{H}_5\cdot$ (-H)	252	benzo[e]pyrene	 (-H <sub>2</sub> )
166	fluorene	 (-H <sub>2</sub> )	254	phenylphenanthrene	 + $\text{C}_6\text{H}_5\cdot$ + $\text{C}_6\text{H}_4\cdot$ (-H)
168	diphenylmethane	 + $\text{C}_6\text{H}_5\cdot$ (-H)	302	dibenzo[fg,op]naphthacene	 (-H <sub>2</sub> )
176	pyracylene	 + $\equiv$ (-H <sub>2</sub> )	304	phenyltriphenylene	 + $\text{C}_6\text{H}_5\cdot$ + $\text{C}_6\text{H}_4\cdot$ (-H)
178	phenanthrene	 (-2H <sub>2</sub> )			
		 + $\equiv$ (-H <sub>2</sub> )			
182	bibenzyl	2 			
192	methylphenanthrene	 + CH <sub>3</sub>			
202	fluoranthene	 (-H <sub>2</sub> )			

**Figure 5.** Corannulene structure as a part of C<sub>60</sub>.

TOFMS method and were compared with those of toluene only. The results are summarized as follows.

(1) When benzene was added, a significant increase of phenyl addition products (biphenyl, terphenyl, and triphenylene) together with the increase of larger PAHs was observed. (2) A clear regular sequence of mass spectra was observed with an interval of  $\sim 74$  mass numbers ( $+\text{C}_6\text{H}_5 - 3\text{H}$ ). (3) The analysis showed that the PAC growth is efficient for PAHs without triple fusing site, for which HACA is inefficient, and produces and grows PAHs with five-membered rings.

The growth mechanism observed for large PAHs seems to be applicable for other combustion or pyrolysis conditions, and

roles of PAC together with other growth mechanisms (HACA and CPDR) and roles of PAHs with five-membered rings produced by PAC were discussed.

## References and Notes

- (1) (a) Haynes, B. S.; Wagner, H. Gg. *Prog. Energy Combust. Sci.* **1981**, *7*, 229. (b) Homann, K. H. *Proc. Combust. Inst.* **1984**, *20*, 857. (c) Howard, J. B. *Proc. Combust. Inst.* **1990**, *23*, 1107. (d) Bockhorn, H., Ed. *Soot Formation in Combustion: Mechanisms and Models*; Springer-Verlag: Berlin, 1994. (e) Glassman, I. *Combustion*; Academic Press: San Diego, 1996. (f) Frenklach, M. *Phys. Chem. Chem. Phys.* **2002**, *4*, 2028–2037.
- (2) Appel, J.; Bockhorn, H.; Frenklach, M. *Combust. Flame* **2000**, *121*, 122.
- (3) (a) Richter, H.; Howard, J. B. *Prog. Energy Combust. Sci.* **2000**, *26*, 565. (b) Homann, K. H. *Angew. Chem.* **1998**, *110*, 2572. (c) Goldaniga, A.; Faravelli, T.; Ranzi, E. *Combust. Flame* **2000**, *122*, 350.
- (4) (a) Howard, J. B.; Bittner, J. D. *Proc. Combust. Inst.* **1980**, *18*, 1105. (b) Homann, K.-H.; *Proc. Combust. Inst.* **1990**, *23*, 857. (c) Sarofim, A. F.; Masonjones, M. C. *Chem. Phys. Processes Combust.* **1995**, *1*, 265. (d) Weilmunster, P.; Keller, A.; Homann, K. *Combust. Flame* **1999**, *116*, 62.
- (5) Bockhorn, H.; Fetting, F.; Wenz, H. W.; *Ber. Bunsen-Ges. Phys. Chem.* **1983**, *87*, 1067.
- (6) Frenklach, M.; Clary, D. W.; Gardiner, W. C.; Stein, S. E. *Proc. Combust. Inst.* **1984**, *20*, 887.
- (7) Bohm, H.; Jander, H.; Tanke, D. *Proc. Combust. Inst.* **1998**, *27*, 1605–1612.
- (8) McKinnon, J. T.; Howard, J. B. *Proc. Combust. Inst.* **1992**, *24*, 965–971.

(9) (a) Mathieu, O.; Frache, G.; Djebaili-Chaumeix, N.; Pillard, C. E.; Krier, G.; Muller, J. F.; Douce, F.; Manuelli, P. *Proc. Combust. Inst.* **2006**, *31*, 511–519. (b) Dobbins, R. A.; Fletcher, R. A.; Chang, H. C. *Combust. Flame* **1998**, *115*, 285–298. (c) Dobbins, R. A.; Fletcher, R. A.; Lu, W. *Combust. Flame* **1995**, *100*, 301–309. (d) Keller, A.; Kovacs, R.; Homann, K. -H. *Phys. Chem. Chem. Phys.* **2002**, *2*, 1667–1675.

(10) (a) Badger, G. M. *Prog. Phys. Org. Chem.* **1965**, *3*, 1–40. (b) Badger, G. M.; Donnelly, J. K.; Spotswook, T. M.; *Aust. J. Chem.* **1964**, *17*, 1147–1156. (c) Sarofim, A. F.; Longwell, J. P.; Wornat, M. J.; Mukherjee, J. *Springer* 1994, 485–500. (d) Griesheimer, J.; Homann, K. -H. *Proc. Combust. Inst.* **1998**, *27*, 1753–1761. (e) Dong, G. L.; Huttinger, K. J. *Carbon* **2002**, *40*, 2515–2528.

(11) Unterreiner, V. B.; Sierka, M.; Ahlrichs, R. *Phys. Chem. Chem. Phys.* **2004**, *6*, 4377–4384.

(12) (a) Marinov, N. M.; Pitz, W. J.; Westbrook, C. K.; Castaldi, M. J.; Senkan, S. M. *Combust. Sci. Technol.* **1996**, *116/117*, 211. (b) Richter, H.; Grieco, W. J.; Howard, J. B. *Combust. Flame* **1999**, *119*, 1–22.

(13) Shukla, B.; Susa, A.; Miyoshi, A.; Koshi, M. *J. Phys. Chem. A* **2007**, *111*, 8308–8324.

(14) (a) Wang, H.; Frenklach, M. *Combust. Flame* **1997**, *110*, 173. (b) Aguilera-Ipanragirre, J.; Klopper, W. *J. Chem. Theory Comput.* **2007**, *3*, 139–145.

(15) Müller, J.-O.; Su, D. S.; Wild, U.; Schlögl, R. *Phys. Chem. Chem. Phys.* **2007**, *9*, 4018–4025.